Biophysical Chemistry 9 (1979) 97–103

DETERMINATION OF POLYMER SIZE DISTRIBUTION BY COMBINATION OF QUASIELASTIC LIGHT SCATTERING AND BAND TRANSPORT: EVALUATION OF THE EFFECT OF DIFFUSION

G.J. WEI and Victor A. BLOOMFIELD
Department of Biochemistry, University of Minnessota, St. Paul, Minnessota 55108, USA

Received 6 July 1978

In this paper we report a computer simulation study of the effect of diffusion on the size distribution obtained by combining light scattering with isokinetic band sedimentation or electrophoresis. We find that, under typical experimental conditions, the method yields reasonably accurate size distributions for samples of particles greater than 10 nm radius. However, caution should be exercised in interpreting the results for smaller particles, for which the distortion due to diffusion can be considerable.

1. Introduction

Polydispersity often complicates interpretation of physical measurements on polymer solutions. While it is possible to gain valuable information from various average properties (number average, weight average, *Z*-average, etc.) more detailed characterization of sample heterogeneity is generally desirable. If a few moments of a molecular weight or size distribution are measured, the parameters of an assumed functional form of the distribution may be determined. Such a procedure is rarely justified, however, unless supplementary information validating the assumed form of the distribution is available, or unless a large number of moments (more than the two or three usually measured) can be determined and shown to be mutually consistent.

Therefore, physical separation, for example, by gel filtration or differential centrifugation, or other approaches, such as electron microscopy or Coulter counting, for quantitating and characterizing individual species in a polydisperse solution are often desirable. A recently developed approach that shows considerable promise is to spread an initially thin band of sample by applying an electrophoretic [1] or centrifugal [2] field. After sufficient translational dispersion of the various components of the band has occurred, a laser beam is scanned along the transport cell. The macromolecular concentration in each solution segment is determined from the total intensity of scattered light, and the average hydrodynamic radius by quasielastic light scattering (QLS). A plot of size versus concentration then gives the desired size distribution curve which is readily converted to a molecular weight distribution. This method is relatively convenient, and is accurate and capable of high resolution when diffusional spreading can be neglected [3].

It is easy to see, however, that if the rate of diffusional spreading is comparable to the transport rate, the distribution may be distorted from its true shape. At any given point, the molecules found will be not only those predicted to have reached that point on the basis of their sedimentation coefficients or electrophoretic mobilities, but also those that have diffused to that point from neighboring predicted positions.

In this paper we report a computer simulation study of the effect of diffusion on the size distribution obtained by combining light scattering and QLS with isokinetic band sedimentation or electrophoresis. We find that, under typical experimental conditions, the method yields reasonably accurate size distributions for samples of particles greater than 10 nm radius. However, caution should be exercised in interpreting the results for smaller particles, for which the distortion due to diffusion can be considerable.

2. Methods

Computer simulation is carried out for the three physical processes involved in this method: (a) isokinetic band transport for a time t in a stabilizing gradient to achieve spatial dispersion along the transport axis x; (b) total intensity light scattering $I(x, t)$ to get the product of the local total concentration $C(x)$ and weight-averaged molecular weight $M_w(x)$; and (c) quasielastic light scattering to get the Stokes radius $R(x)$. The size distribution is then obtained by dividing $R(x)^3$ into $I(x, t)$ to get a quantity proportional to $C(R)$ and plotting against R.

2.1. Isokinetic band transport

A thin band of sample is caused to move and spread in a centrifugal or electric field until suitable separation of the band components is achieved. The time required for the spreading, t, is calculated from:

$$t = d/[V(R_{max}) - V(R_{min})], \quad (1)$$

where d is the separation between the largest (R_{max}) and the smallest (R_{min}) particles, and $V(R)$ is the velocity of the particles of size R.

All particles are assumed to behave independently, so that Fick's law of diffusion applies. In an ideal case where the initial band is infinitely thin (a delta function in x), the spatial distribution of particles with size R at time t would be:

$$C(x, R, t) = \{f(R)/[4\pi D(R)t]^{1/2}\} \times \exp\{-[x - x^*(R, t)]^2/4D(R)t\}, \quad (2)$$

where $f(R)$ is the size distribution of the sample, $x^*(R, t)$ is the position of the center of the gaussian band formed by particles of size R, and $D(R)$ is the diffusion coefficient of particles of size R.

In practical cases, the initial band is of finite width L, and may be treated as a group of adjacent delta-functions. Then the distribution at time t is obtained by integrating eq. (2) over the initial band:

$$C(x, R, t) = \int_{-L/2}^{L/2} \{f(R)/[4\pi D(R)t]^{1/2}\} \times \exp\{-[x - x^*(R, t) - \psi]^2/4D(R)t\}\, d\psi. \quad (3)$$

Without losing generality we fix the origin of x at the center of the initial band, and the parameter $x^*(R, t)$ is simply

$$x^*(R, t) = V(R)t. \quad (4)$$

In the case where centrifugal field is used to achieve spatial separation,

$$V(R) = \tfrac{2}{9}(\rho_p - \rho_s)(g/\eta)R^2, \quad (5)$$

where ρ_p and ρ_s are, respectively, the densities of the particles and the solution, g is the average centrifugal field, and η is the viscosity of the solution. Two assumptions are involved in using eq. (5). First, the shape of particles is spherical; and second, the stabilizing gradient is isokinetic, so that the changes in viscosity, density, and accelerating field across the centrifuge tube compensate each other.

If an electric field is used in place of the centrifugal field,

$$V(R) = \{Z(R)eE/6\pi\eta R\}\phi(KR), \quad (6)$$

where $Z(R)$ is the particle charge, e is the proton charge, E is the applied electric field, and $\phi(KR)$ is a correction factor depending on ionic strength through the Debye-Hückel inverse length K.

In this study, simulation is done only for the case of centrifugal fields. However the effect of diffusion on the observed size distribution should be similar for both cases.

2.2. Total intensity light scattering

The intensity of scattered light is proportional to the product of the weight concentration and the molecular weight:

$$I(x, t) = \int_{R_{min}}^{R_{max}} M(R)\, C(x, R, t)\, P(\theta, R)\, dR, \quad (7)$$

$$P(\theta, R) \approx 1 - (16\pi^2\tilde{n}R^2/5\lambda^2)\sin^2\theta/2 \quad \text{for uniform spheres,} \quad (8)$$

where $P(\theta, R)$ is the form factor (which corrects for the internal interference when R is not much smaller than λ), λ the wavelength of laser light, $\tilde{n}$ the refractive index, and θ the scattering angle.

Because the observing window is not infinitesimal, the observed intensity of scattering, $I'(x, t)$, is actually

an average over the segment of sample being observed:

$$I'(x,t) = \int_{x-W/2}^{x+W/2} I(x',t)\,dx', \tag{9}$$

where W is the width of the window.

2.3. Quasielastic light scattering

It has been shown that the autocorrelation function of the photocurrent may be analyzed by the cumulant expansion method [4] to get the Z-averaged diffusion coefficient:

$$D_Z(x) = \int_{R_{min}}^{R_{max}} \frac{D(R)M(R)C(x,R,t)P(\theta,R)\,dR}{I(x,t)} \tag{10}$$

Again, when the size of the observation window is taken into account,

$$D'(x) = \int_{x-W/2}^{x+W/2} D_Z(x')\,dx'/W. \tag{11}$$

2.4. Size distribution

Applying the Stokes-Einstein equation, the average hydrodynamic radius of the particles at x will be

$$R'(x) = kT/6\pi\eta D'(x), \tag{12}$$

where k is the Boltzmann constant and T the temperature. The distribution function determined by this method is then:

$$f'(R) = I'(x,t)/\{[R'(x)]^3 P(\theta,R')\}. \tag{13}$$

For the purpose of comparison, the distribution function based on the true size, $R(x)$, is also computed:

$$f''(R) = I'(x,t)/\{[R(x)]^3 P(\theta,R)\}. \tag{14}$$

$R(x)$ is determined from eq. (4) relating x and t to $V(R)$. All distribution functions are normalized to unity before comparison.

2.5. Values of parameters

The Schulz-Zimm [5,6] molecular weight distribution function, $F(M)$, was used to generate input size distribution functions, $f(r)$:

$$F(M) = M^z y^{z+1} e^{-yM}/\Gamma(z+1), \tag{15}$$

$$f(R) = F(\tfrac{4}{3}\pi R^3 \rho_P), \tag{16}$$

where $y = (\overline{M_w} - \overline{M_n})$, $z = y\overline{M_n}$ and $\Gamma(z+1)$ is the gamma function. The parameters y and z are varied to produce distributions of different size ranges and widths.

The values of other parameters were carefully selected to imitate practical experimental conditions and were held unchanged throughout this study. They are:

L = initial band width = 0.1 cm,
W = window of observation = 0.01 cm,
ρ_p = density of the sample particles = 1.3 g/ml,
ρ_s = density of the solution = 1.0 g/ml,
η = viscosity of the solution = 1.0 centipoise,
g = average centrifugal field = 1.75×10^7 cm/s^2,
T = temperature = 293.15 K,
d = maximum separation = 2 cm,
λ = wavelength of laser light = 5145 Å,
θ = scattering angle = 60 degrees,
$\tilde{n}$ = refractive index = 1.33.

2.6. Computer simulation

The x coordinate is quantized in segments of 0.004 cm. The error function resulting from eq. (3) was evaluated by table searching and linear interpolation to save computing time. The cutoff of the table is set at 2.5 (in units of standard deviation), which corresponds to a maximum error of 0.6% in the final value of the error function. This cutoff point sets the range of summation (eqs. (7) and (10)) in the computer program:

$$\left|\frac{x - x^* \pm L/2}{[2D(R)t]^{1/2}}\right| \leqslant 2.5. \tag{17}$$

3. Results

Fig. 1a shows a typical simulation of the apparent size distribution, $f'(R)$, as obtained by light scattering and band sedimentation. The input distribution, $f(R)$, is also plotted (in dashed line) for comparison. At the top is a plot of the 3× magnified difference between the two. It is seen that the size distribution

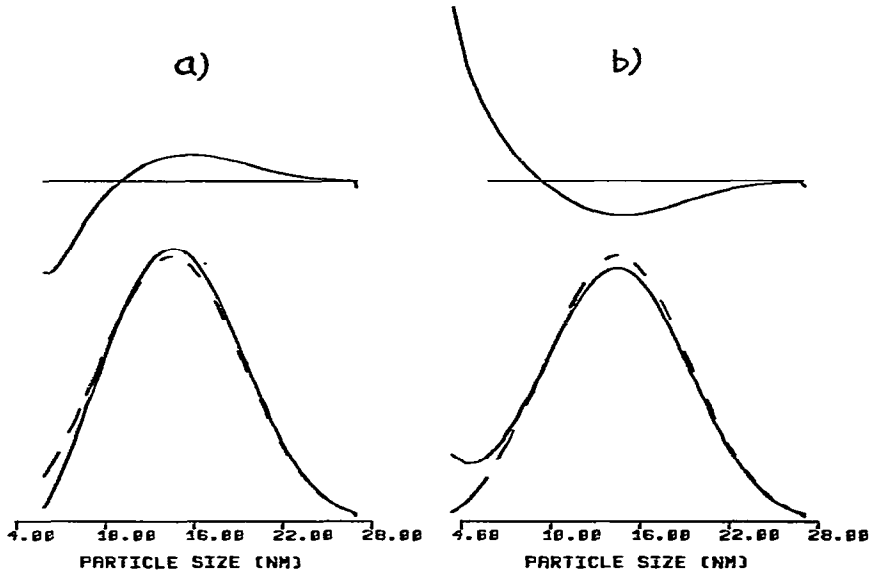

Fig. 1. Size distribution obtained by simulated sedimentation and quasi-elastic light scattering (solid line), model input distribution (dashed line), and magnified (3X) difference (at top). Input parameters are $z = 1, y = 1 \times 10^7$. The ordinate is the weight concentration in arbitrary units. (a) Particle sizes determined by QLS. (b) Particle sizes based on the distance travelled during centrifugation.

from the light scattering experiment yields too small a concentration for smaller particles, and slightly too large a concentration for the median sized, and reproduces almost exactly that of the larger particles. These deviations come from both the total intensity scattering and the QLS measurements. To apportion the relative contribution between the two, a plot of the distribution function based on the "true" size, R (calculated from the distance sedimented, i.e. assuming no diffusion has occurred) is shown in fig. 1b. The difference curve (at top) shows an opposite trend and has a similar magnitude to that of fig. 1a. This indicates that the deviation due to the size measurement is larger than that due to the total intensity measurement, a fact which is not entirely surprising because the mixing due to the diffusion process is expected to increase the average size measured by QLS for the smaller particles and this effect is cubed in calculating $f'(R)$ from eq. (13).

It is interesting to observe that the size of smaller particles as determined directly from the sedimentation distance is too small, causing the observed distribution to show positive deviation (the left end of fig. 1b).

Fig. 2 shows the results of a series of computations with the Schulz-Zimm parameters y and z varied to cover the range of sizes from 2 nm to 100 nm. It can be seen that the degree of distortion increases with decreasing particle size and increasing sample breadth. The standard deviation of the observed distribution from the input distribution for each set of runs is listed in table 1 as a measure of the resemblance between the two. A general conclusion can be derived from fig. 2 and table 1: the distribution function by sedimentation and light scattering is a good approximation (within a standard deviation of 2%) to the true distribution provided that the size (radius) of the particles in the sample is larger than 10 nm and that the distribution is not too broad.

However for samples with size smaller than 10 nm, the distortion can be substantial as evidenced by fig. 3. The peak position is shifted toward the high molecular weight side by 0.32 nm, approximately 14% of the half width, and the standard deviation is as high as 19%.

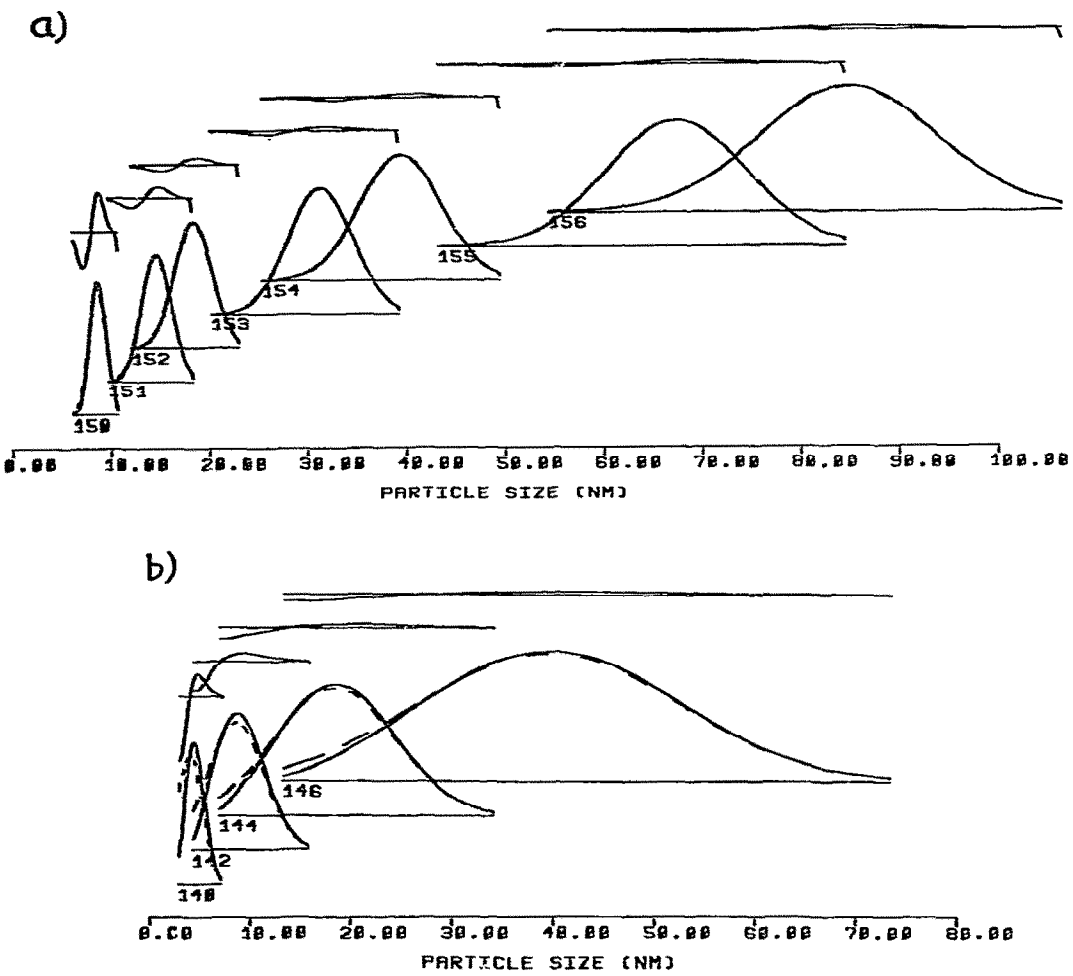

Fig. 2. Observed weight concentrations versus particle sizes (solid line) for various model inputs (dashed line). The Schulz-Zimm parameters for the input distributions are listed in table 1. Magnifications for the difference curves (at top) are 5.0 for (a), and 1.0 for (b). The peak heights of all distributions are normalized to the same arbitrary value.

A form factor correction based on the size determined from QLS improves the result by shifting the distribution towards larger size, as illustrated in fig. 4. The correction itself can be substantial (34% for a sphere of 80 nm radius under the conditions used in this study). But normalization of the area under the distribution to unity tends to minimize the final effect. Eq. (8) would not be a good approximation when $(4\pi\tilde{n}R/\lambda)\sin\theta/2$ is large compared to unity. Therefore, one has to include higher order terms in eq. (8) for samples of large particles.

4. Discussion

The physical phenomena modelled in this simulation are all well understood. Therefore it is reasonable to assume that the simulation leads to results bearing

Table 1
Standard deviation between the measured and model input distributions

run no.	z [a]	y [a] ($\times 10^7$)	size (nm)	t [b] (min)	% standard deviation [c]
140	1	50	0.9– 7.4	530	19.0
141	1	10	1.5–12.6	182	10.0
142	1	5	1.8–15.9	114	7.3
143	1	1	3.1–27.2	39	3.4
144	1	0.5	4.0–34.3	25	2.6
145	1	0.1	6.8–58.7	8	1.8
146	1	0.05	8.5–73.9	5	1.7
150	10	50	5.3–10.7	331	3.8
151	10	10	9.1–18.3	113	1.0
152	10	5	11.5–23.1	71	0.67
153	10	1	19.6–39.4	24	0.38
154	10	0.5	24.7–49.7	15	0.35
155	10	0.1	42.2–84.9	5	0.33
156	10	0.05	53.1–107.0	3	0.32

[a] Schulz-Zimm parameters, see eq. (15).
[b] Time required for the initial band to spread out to d cm.
[c] Standard deviations as a percentage of maximum peak height.

a close resemblance to what would happen in real experiments.

The Schulz-Zimm distribution function was arbitrarily chosen as a model input size distribution The key problem in interpreting results originates from diffusion process. Consequently the choice of model input distribution should not alter the general conclusions.

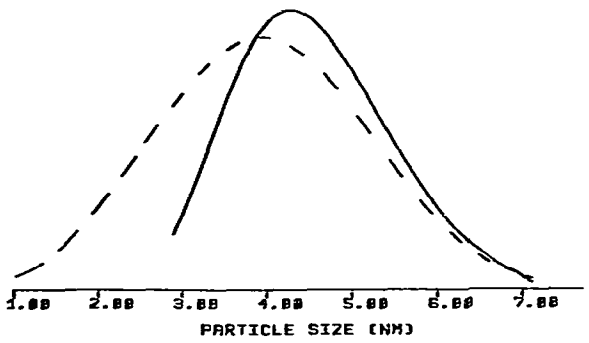

Fig. 3. Distortion due to diffusion can be considerable when the particle size is small. The apparent distribution is plotted as a solid line, and the true distribution as a dashed line. For parameters, see run no. 140 in table 1.

Other parameters have small effects on the results. Thinner initial band L, wider separation d, greater centrifugal field, lower temperature, and smaller window of observation W all tend to improve the accuracy of the results. However, they are not expected to introduce significant changes as long as they are kept close to ordinary experimental conditions. The initial band width of 1 mm can be easily obtained experimentally. The centrifugal field of 1.75×10^7 cm/s^2, corresponding to 14 000 rpm for a radial distance of 8 cm, is typically within the range of an ordinary centrifuge. The observation window of 0.01 cm roughly corresponds to the diameter of a focused laser beam. (The window size is adjustable by the pin hole in front of the photomultiplier. The beam size is usually the upper limit of the window). A separate series of computations with $z = 1$ was done for the case where the observation window is 0.03 cm. No differences in results were apparent despite the three fold change in window size.

In a very recent paper of Kunitake et al. [7], light scattering and centrifugation were used to obtain the distributions of molecular weight, size, density and frictional coefficient for very low density lipoproteins. The observed size distribution was compared with the results from electron microscopy in their fig. 7. While

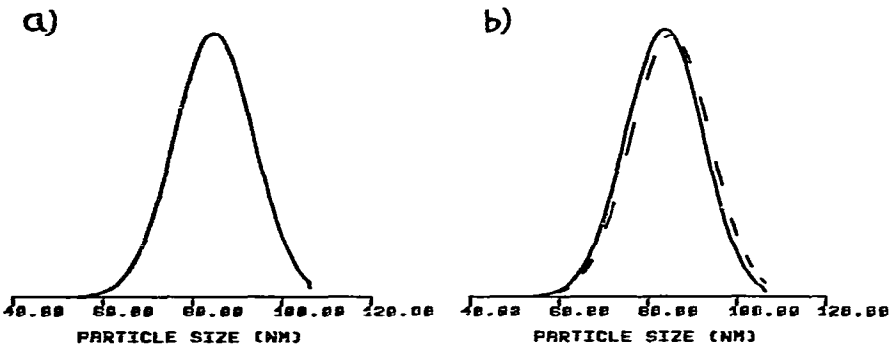

Fig. 4. Effect of form factor correction. (a) corrected (eq. (13) used as shown). (b) uncorrected (eq. (13) used without the form factor correction $P(\theta, R)$. See run no. 156 of table 1 for the parameters used.

the overall agreement is remarkable, the method of combining light scattering with centrifugation seems to underestimate the concentration of smaller particles (200–500 Å). This is in agreement with our prediction that underestimation of small particles may result from neglect of diffusion.

The conclusions drawn from this study should be applicable to other techniques, which differ only in the means of achieving spatial dispersion of the initial sample band. Among these are QLS-electrophoresis and QLS-gel filtration.

Acknowledgements

This research was supported in part by NIH grant GM 17855.

References

[1] T.K. Lim, G.J. Baran and V.A. Bloomfield, Biopolymers 16 (1977) 1473.
[2] D.E. Koppel. Biochemistry 13 (1974) 2712.
[3] T.K. Lim, V.A. Bloomfield and G. Krejcarek, in preparation.
[4] D.E. Koppel, J. Chem. Phys. 57 (1972) 4814.
[5] G.V. Schulz, Z. Physik. Chem. B43 (1939) 25.
[6] B.H. Zimm, J. Chem. Phys. 16 (1948) 1099.
[7] S.T. Kunitake, F. Loh, V.N. Schumaker, S.K. Ma, C.M. Knobler, J.P. Kane and R.L. Hamilton, Biochemistry 17 (1978) 1936.